Available online at www.sciencedirect.com
SCIENCE DIRECT®
Bioorganic & Medicinal Chemistry Letters
Bioorganic & Medicinal Chemistry Letters 14 (2004) 5357–5366

In vitro plasma protein binding and aqueous aggregation behavior of astaxanthin dilysinate tetrahydrochloride

Ferenc Zsila,[a] Ilona Fitos,[a] Zsolt Bikádi,[a] Miklós Simonyi,[a] Henry L. Jackson[b] and Samuel F. Lockwood[b,*]

[a]*Institute of Biomolecular Chemistry, Chemical Research Center, Budapest, PO Box 17, H-1525, Hungary*
[b]*Hawaii Biotech, Inc., 99-193 Aiea Heights Drive, Suite 200, Aiea, HI 96701, USA*

Received 2 July 2004; revised 6 August 2004; accepted 6 August 2004
Available online 3 September 2004

Abstract—The tetrahydrochloride salt of astaxanthin di-L-lysinate (lys_2AST) is a highly water-dispersible astaxanthin–amino acid conjugate, with an aqueous dispersibility of $\geqslant$181.6 mg/mL. The statistical mixture of stereoisomers has been well characterized as an aqueous-phase superoxide anion scavenger, effective at micromolar (μM) concentrations. In the current study, the aqueous aggregation behavior and in vitro plasma protein binding [with fatty-acid-free human serum albumin (HSA) and α_1-acid glycoprotein (AGP)] were investigated with a suite of techniques, including circular dichroism (CD) and UV–vis spectroscopy, ultrafiltration, competitive ligand displacement, and fluorescence quenching. Induced CD bands obtained in Ringer buffer solution of HSA demonstrated high affinity monomeric binding of the compound at low ligand per protein (*L*/*P*) ratios (in aqueous solution alone the carotenoid molecules formed card-pack aggregates). The binding constant ($\sim 10^6\,M^{-1}$) and the binding stoichiometry (~0.2 per albumin molecule) were calculated from CD titration data. CD displacement and ultrafiltration experiments performed with marker ligands of HSA indicated that the ligand binding occurred at a site distinct from the main drug binding sites of HSA (i.e., Sites I and II). At intermediate *L*/*P* ratios, both monomeric and aggregated ('chirally complexed') binding occurred simultaneously at distinct sites of the protein. At high *L*/*P* ratios, chiral complexation predominantly occurred on the asymmetric protein template. The tentative location of the chirally-complexed aggregation on the HSA template was identified as the large interdomain cleft of HSA, where carotenoid derivatives have been found to bind previously. Only weak binding to AGP was observed. These results suggest that parenteral use of this highly potent, water-dispersible astaxanthin–amino acid conjugate will result in plasma protein association, and plasma protein binding at sites unlikely to displace fatty acids and drugs bound at well-characterized binding sites on the albumin molecule.

1. Introduction

The C_{40} carotenoids—of which β-carotene and lycopene ('carotenes'), as well as lutein, zeaxanthin, and astaxanthin ('xanthophylls') are prototypes—are potent biological antioxidants that are practically insoluble in water.[1] Of the greater than 700 described naturally-occurring carotenoids, the vast majority have limited or undetectable solubility in aqueous solution.[2] To increase the utility of these compounds for evaluation in aqueous-phase model systems and potential clinical applications, various techniques have been utilized to increase the solubility and/or dispersibility in various vehicles.[3–5] Recently, investigations of the synthesis and characterization of water-soluble and water-dispersible C_{30} and C_{40} carotenoid derivatives have appeared.[6–13] A critical first step in the evaluation of the utility of these compounds in aqueous applications is the assessment of radical scavenging behavior in aqueous solution.[7] Due to their large hydrophobic surfaces, carotenoid molecules readily form self-assemblies in an aqueous environment. If such assemblies are built up by chiral monomers, they often exhibit strong excitonic-type CD activity, which originates from the excited state coupling of the neighboring chirally-arranged polyene chains.[14,15]

Abbreviations: α_1-Acid glycoprotein, AGP; astaxanthin di-L-lysinate tetrahydrochloride, lys_2AST; circular dichroism, CD; Cotton effect, CE; disodium disuccinate derivative of *meso*-astaxanthin, dAST; human serum albumin, HSA; ligand/protein molar ratio, *L*/*P*; ultraviolet–visible, UV–vis.

Keywords: α_1-Acid glycoprotein; AGP; Astaxanthin; Astaxanthin di-L-lysinate tetrahydrochloride; Card-pack aggregation; Carotenoid derivatives; Chiral complexation; Circular dichroism spectroscopy; Human serum albumin; HSA; Induced chirality.

* Corresponding author. Tel.: +1 808 220 9168; fax: +1 808 792 1343; e-mail: slockwood@hibiotech.com

0960-894X/$ - see front matter © 2004 Elsevier Ltd. All rights reserved.
doi:10.1016/j.bmcl.2004.08.013

Supramolecular helicity of these aggregates is governed by noncovalent intermole- cular interactions that have arisen between the chiral end groups of the monomers. Achiral carotenoid compounds show no optical activity either in molecular or aggregated states, however, definite supramolecular chirality can be detected if the molecules aggregate on an asymmetric template—for example, a protein surface—where the chiral environment initiates and sets the handedness of the helical stacking of carotenoid molecules.[8] Thus, after investigation of supramolecular assemblies of carotenoid derivatives in aqueous formulations, a logical second step is an assessment of the plasma protein binding of these compounds in vitro, prior to parenteral administration in relevant animal models. In certain cases, aqueous dispersibility achieved by supramolecular assembly may be viewed as an artifact of aqueous formulation; an immediate and preferential binding to human serum albumin (HSA), the most abundant protein in mammalian blood, makes parenteral applications relevant and successful.[9]

In the current study, the binding of astaxanthin di-L-lysinate tetrahydrochloride (the statistical mixture of stereoisomers, lys_2 AST) to the two main human serum proteins—albumin (HSA) and α_1-acid glycoprotein (AGP)—was studied by circular dichroism (CD), ultraviolet–visible (UV–vis), and fluorescence spectroscopic methods. Competitive displacement binding studies were also undertaken with model ligands with known and well-characterized binding sites on HSA. Strong binding to HSA at a binding site discrete from the two main drug binding sites (Sites I and II)[16] was observed; only weak binding to AGP was noted. Comparison with similar data obtained for a novel anionic C_{40} bolaamphiphilic derivative[8] suggests that an increased strength of association was noted for the cationic derivative in the current study, attributed at least in part to the nature of the L-lysine moieties in the conjugated compound.

In addition, the aqueous aggregation behavior of lys_2AST was also investigated using chiroptical spectroscopy. The synthesis, characterization, and superoxide scavenging (in an aqueous model system) of this novel C_{40} carotenoid derivative had been described previously.[13] Preliminary evidence, utilizing UV–vis spectroscopy, had been obtained in that study on the probable H-type ('card-pack') time-dependent aggregation of the compound in aqueous formulation.

2. Ligand test material

Nonesterified astaxanthin (as the statistical mixture of stereoisomers 3*S*,3′*S*, *meso*-3*R*,3′*S*, and 3*R*,3′*R* in a 1:2:1 ratio; Buckton Scott, India; Fig. 1a) was used as starting material for the synthesis of astaxanthin di-L-lysinate tetrahydrochloride (lys_2AST) (Fig. 1b) by Hawaii Biotech, Inc.; methods for synthesis and characterization have been published previously.[13] The test compound also consists of a mixture of stereoisomers lacking optical activity. The purity had been determined by HPLC as 97.0% (as area under the curve, AUC).

3. Other chemicals

Fatty-acid-free HSA (Sigma), HSA-fraction V (Sigma), AGP (Sigma), (*rac*)-warfarin (Fig. 2), *rac*-[^{14}C]warfarin (2.07 GBq/mmol, Amersham Pharmacia Biotech), *rac*-flurbiprofen (Sigma), palmitic acid (Sigma), sodium (Na)-salicylate (Reanal, Hungary), buffer constituents

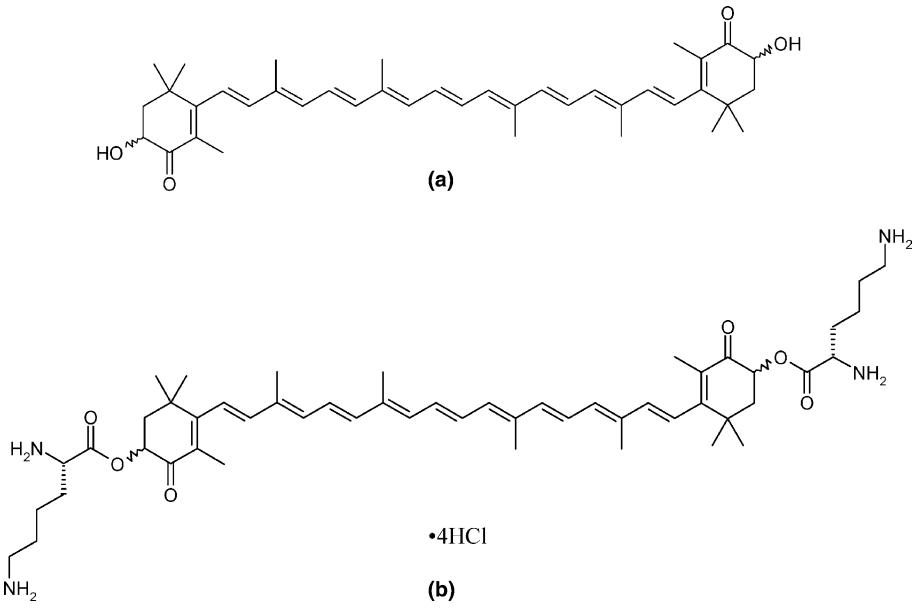

Figure 1. Chemical formulae of (**a**) nonesterified astaxanthin (3,3′-dihydroxy-β,β-carotene-4,4′-dione) utilized as a synthetic scaffold for retrometabolic (i.e., 'soft-drug') synthesis of (**b**) lys_2AST utilized in the current study. The compound is supplied commercially as the 'racemate' (i.e., statistical mixture of stereoisomers 3*S*,3′*S*, *meso*-3*R*,3′*S*, and 3*R*,3′*R* in a 1:2:1 ratio).

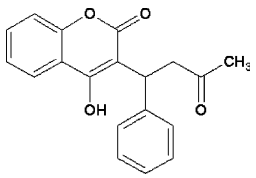

Figure 2. Chemical formula of *rac*-warfarin used as a model ligand in the current study. *rac*-Warfarin is a marker of drug binding to Site I of HSA.

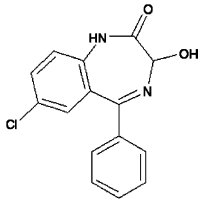

Figure 3. Chemical formula of *rac*-oxazepam used as synthetic scaffold for generation of hemisuccinate[17] used as a model ligand in the current study. (*S*)-Oxazepam hemisuccinate (diazepam analog) is a marker of drug binding to Site II of HSA.

(Reanal, Hungary), and organic solvents (HPLC grade) were obtained commercially and used as supplied. *rac*-Oxazepam (Fig. 3) hemisuccinate synthesized as described[17] was used. Binding studies were performed in physiologic (pH 7.4) Ringer buffer.

4. CD measurements

CD and UV–vis spectra were recorded on a Jasco J-715 spectropolarimeter at 37 °C, in a rectangular cell with 10 mm pathlength equipped with magnetic stirring. The spectra were accumulated three times with a bandwidth of 1.0 nm. Induced CD spectra were obtained as the difference of spectra of the lys_2AST–protein mixture and that of the protein solution alone. Ellipticities were expressed in millidegrees (mdeg). Ligands (L) were added in small aliquots of stock solutions in dimethyl sulfoxide (DMSO) to protein solutions (P), and the *L*/*P* ratio was recorded.

5. Ultrafiltration

Ultrafiltrations were performed in the Amicon MPS-1 system, using YMT30 membranes at 25 °C. The free fraction of [^{14}C]warfarin was measured by liquid scintillation counting. The free fraction of (*S*)-oxazepam hemisuccinate was determined by HPLC analysis on a Chiral-AGP column [100 × 4 mm internal diameter (i.d.), ChromTech AB, Sweden], using mobile phase of 0.01 M phosphate buffer with 3% acetonitrile.[17]

6. Fluorescence quenching

Fluorescence measurements were obtained in a Shimadzu RF-1501 spectrofluorophotometer at 25 °C. The native tryptophan (Trp) fluorescence of HSA and AGP solutions were measured using excitation and emission wavelengths of 280 and 335 nm, respectively. Carotenoid was added in small aliquots of 3 mM stock solution in DMSO. The quenching effect of the DMSO vehicle alone has been found to be negligible.[8,18]

7. CD spectrum of lys_2AST in ethanol and in buffer solution

Definite Cotton effects with signs and spectral positions strongly resembling those of the sodium salt of 3*S*,3′*S*-astaxanthin bis-hemisuccinate (Lockwood, unpublished data) were obtained after solvation of the test sample in EtOH (Fig. 4). Assuming that the asymmetric centers of the L-lysine moieties have negligible influence on the CD spectrum (which is determined essentially by the absolute configuration of the 3 and 3′ carbon atoms in the astaxanthin chromophore), the lys_2AST mixture contained an excess of the 3*S*,3′*S* stereoisomer in relation to 3*R*,3′*R* stereoisomer content (the *meso* form is optically inactive). This observation was corroborated by UV–vis and CD spectra obtained in Ringer buffer (Fig. 5). The blue-shifted and hypochromic main absorption band of the carotenoid indicated the formation of H-type ('card-pack') aggregate; the appearance of two opposite, rather weak induced CD bands in the principal absorption region proved left-handed chiral organization. It is noteworthy that strictly racemic carotenoid mixtures should not show CD activity in either organic or aqueous solutions.[8]

8. Binding of lys_2AST to human serum albumin

8.1. Investigation by CD and UV–vis spectroscopy

Titration of fatty-acid-free HSA with lys_2AST gave rise to binding-induced Cotton effects between 280 and 570 nm (Fig. 6). Two Cotton bands in the near-UV region were of opposite sign, while a broad negative extrinsic CD band developed in the visible spectral region. The Cotton effects increased with the increasing concentration of ligand, and reached saturation around 0.36 ligand/protein ratio (*L*/*P*). The shape and wavelength position of the absorption band showed no sign(s) of aggregation in the early stages of titration, however, a 10 nm blue shift was observed upon further addition of the ligand. At $L/P > 0.4$ a right-handed exciton couplet developed in the visible spectral region coinciding with the blue-shifted absorption band (Fig. 7). Since this exciton couplet was far more intense and oppositely-signed compared to the one which developed without HSA (Fig. 5), it clearly indicated chiral aggregation of carotenoid ligand molecules on the asymmetric protein host.

Induced Cotton effects characteristic of monomeric carotenoid ligand binding to HSA were also detected when the aggregate-induced exciton couplet appeared (Fig. 7), indicating the co-existence of the HSA-bound monomer with the aggregated form. Only the positive band at 375 nm lost intensity and shifted to lower

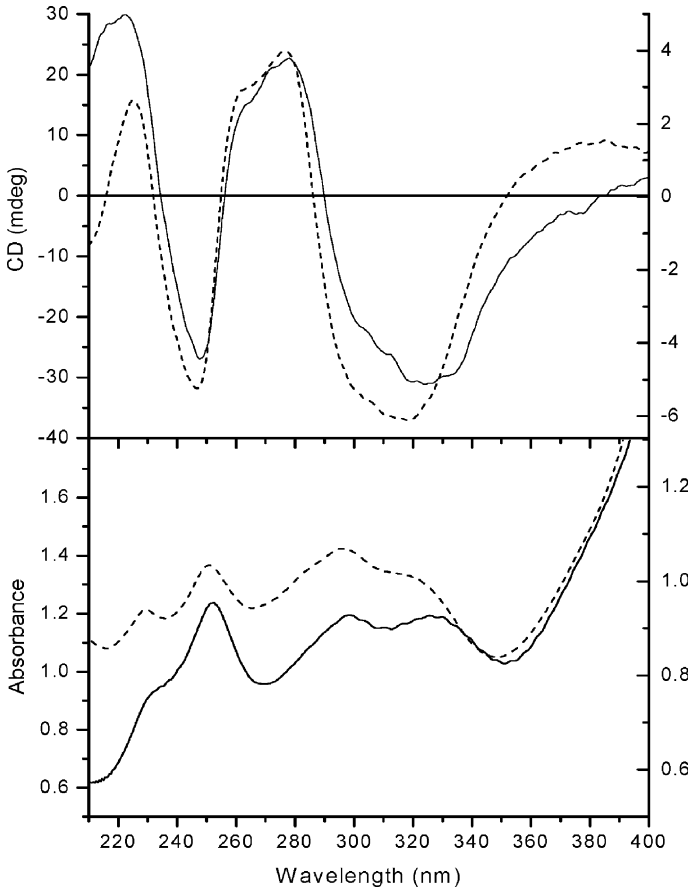

Figure 4. CD and UV spectra of lys_2AST (solid line, right axis, $c = 44.4\,\mu M$) and of 3*S*,3′*S*-astaxanthin disuccinate (dotted line, left axis, $c = 77.3\,\mu M$). lys_2AST was tested as the statistical mixture of stereoisomers in a 1:2:1 ratio (see text). Optical pathlength: 1 cm; solvent: EtOH; temperature: 25 °C.

wavelength due to interference with the neighboring negative exciton band. The molar dichroic absorption coefficients ($\Delta\varepsilon$) of the near-UV CD bands (based on the total concentration of the ligand at the lowest *L*/*P* ratios) were very high, +60 and $-70\,M^{-1}cm^{-1}$ at 374 and 305 nm, respectively.

Since monomeric binding of lys_2AST on HSA showed saturation, the association constant and the binding stoichiometry could be determined. Exploiting the linear part of the binding isotherm, CD values measured at 374 nm (*L*/*P*: 0.04, 0.07, 0.11, and 0.14) were plotted against the concentration of the ligand, and the slope of the resulting line was used to calculate monomer-bound and unbound ratios for higher concentrations. Scatchard plot was constructed (Fig. 8) from which the values of the binding constant (K_a) and number of binding sites (n): $K_a = 2.3 \times 10^6\,M^{-1}$; $n = 0.24$ could be derived. Nonlinear regression analysis, fitting the best curve to experimental near-UV CD band intensities plotted against *L*/*P* ratios (Fig. 9), yielded binding parameters of $1.1 \times 10^6\,M^{-1}$ and 0.20 for K_a and n, respectively. The low value obtained for the number of binding sites suggested that the contribution of one diastereomer only of the lys_2AST mixture dominated in the induced CD spectra; thus, the association constant calculated from the chiroptical data refers to this species only.

9. Binding interaction studies on HSA

9.1. Effect of the lys_2AST on the binding of marker ligands to the two main drug binding sites of HSA evaluated by ultrafiltration

The UV–vis and CD spectra described above indicated that lys_2AST could bind to HSA in monomeric as well as in aggregated forms. Binding studies were performed to determine whether the binding of *rac*-warfarin (marker of drug binding Site I)[19] or (*S*)-oxazepam hemisuccinate (diazepam analog; drug binding Site II marker)[17] to HSA were altered in the presence of lys_2AST.

The binding of 10 μM *rac*-[^{14}C]warfarin to 15 μM HSA was studied in 0.01 M phosphate buffer pH 7.0 at 25 °C. Free fraction values were determined by liquid scintillation counting of ultrafiltrates, as well as of the starting ligand solutions. The free fraction value of the control was 0.22 ± (0.01). In the presence of 20 and 40 μM lys_2-AST, no significant change in free fraction value could be measured. Therefore, it was concluded that the binding of lys_2AST to HSA was independent of drug binding Site I, which is located in subdomain IIA of HSA.

Similarly, the binding of 50 μM *rac*-oxazepam hemisuccinate to 45 μM HSA was studied in Ringer buffer pH 7.4 at 25 °C. Free fraction values were determined

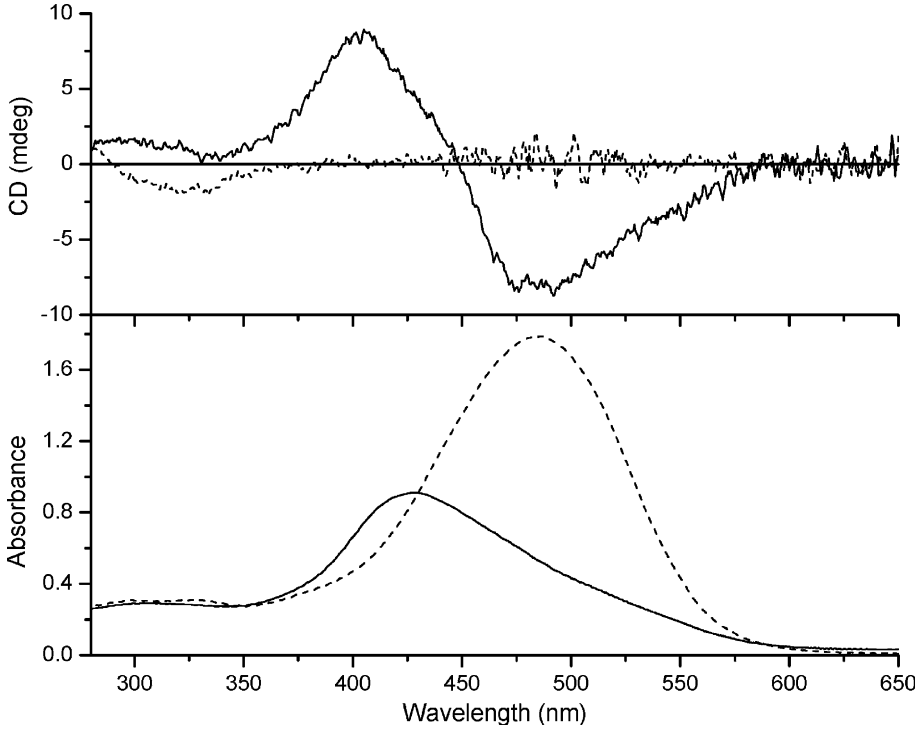

Figure 5. CD and UV–vis spectra of lys_2AST obtained in Ringer buffer (solid line) and EtOH (dotted line); the absorption maximum is blue-shifted from 485.5 nm in EtOH to 428.5 nm in Ringer buffer. Carotenoid concentration is 15.3 μM in both solutions [optical pathlength: 1 cm; temperature: 37 °C; (in EtOH 25 °C)].

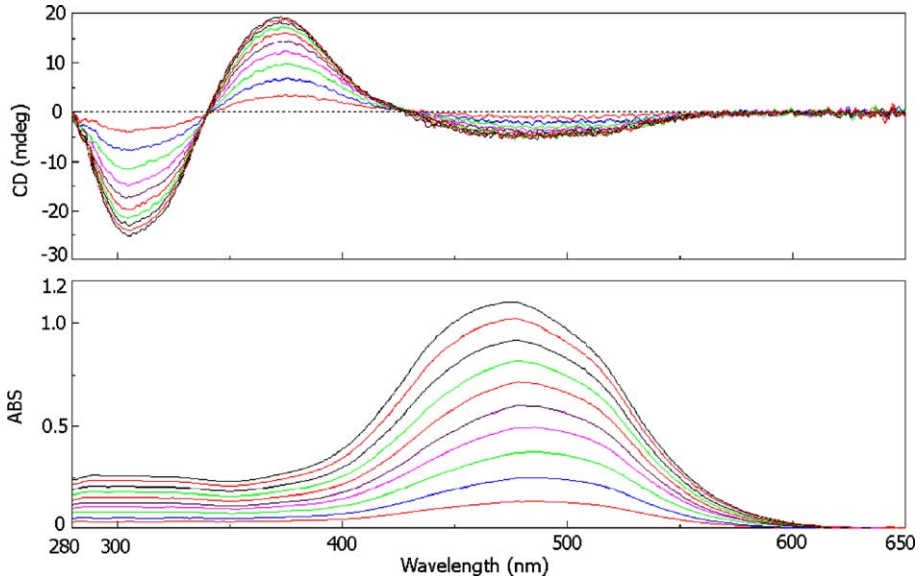

Figure 6. Titration of fatty-acid-free HSA with lys_2AST: part I (*L*/*P* varies from 0 to 0.36). Blue shift of the absorption maxima is seen from 485 to 476 nm as the *L*/*P* ratio increases. The CD bands in Δε units ($M^{-1}cm^{-1}$): +63 and −71 at 374 and 305 nm, respectively (see text). Optical pathlength: 1 cm; temperature: 37 °C; in Ringer buffer (pH 7.4); c_{HSA}: 45 μM; *c*(lys_2AST): from 1.6 to 16.1 μM.

by chiral-HPLC analysis of the ultrafiltrates, as well as of the starting ligand solutions. Since the binding of the (*R*)-enantiomer of oxazepam hemisuccinate is negligible, only the free fraction value of (*S*)-oxazepam hemisuccinate was determined (0.13 ± 0.02) in the starting ligand solution. In the presence of 20, 40, and 80 μM lys_2AST, no significant change in free fraction value could be detected, suggesting that drug binding Site II, located in subdomain IIIA of HSA, is not involved in the lys_2AST–HSA interaction.

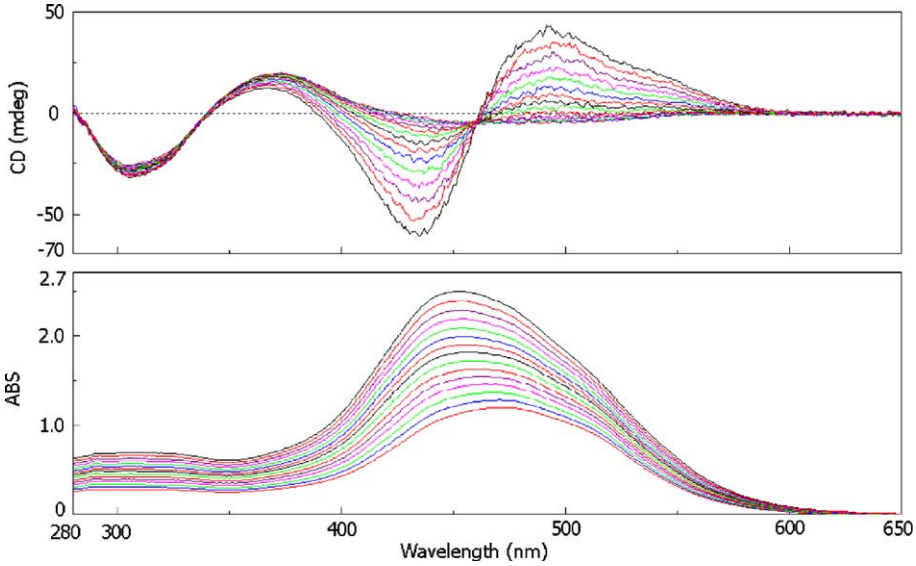

Figure 7. Titration of fatty-acid-free HSA with lys_2AST: part II (*L*/*P* varies from 0.39 to 0.89). Optical pathlength: 1 cm; temperature: 37 °C; in Ringer buffer (pH 7.4). Blue shift of the absorption maxima is seen from 471.5 to 451.5 nm. Positive exciton CD band at 498 nm ($\Delta\varepsilon$: $+27\,M^{-1}cm^{-1}$). Crossover point at 462 nm. Negative exciton CD band at 433 nm ($\Delta\varepsilon$: $-41\,M^{-1}cm^{-1}$). c_{HSA}: 45 μM; $c(lys_2AST)$: from 17.7 to 39.8 μM.

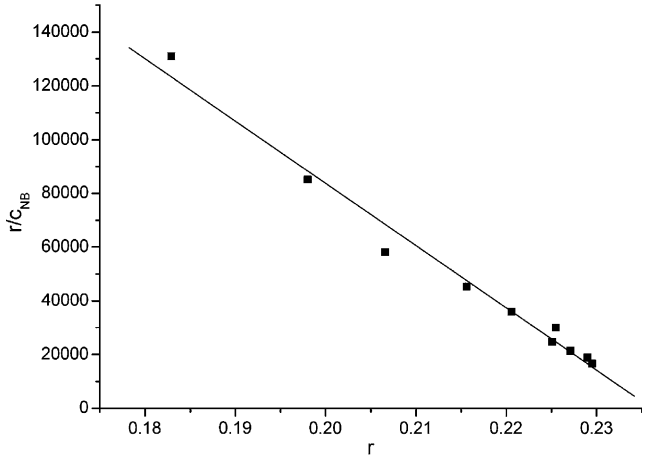

Figure 8. Scatchard plot for monomeric binding of lys_2AST to HSA based on CD titration results (Fig. 6). Key: *r*, the ratio of monomer-bound ligand divided by the concentration of HSA; c_{NB}, concentration of nonbound ligand. Values for the binding constant ($K_a = 2.3 \times 10^6\,M^{-1}$) and number of binding sites ($n = 0.24$) are derived.

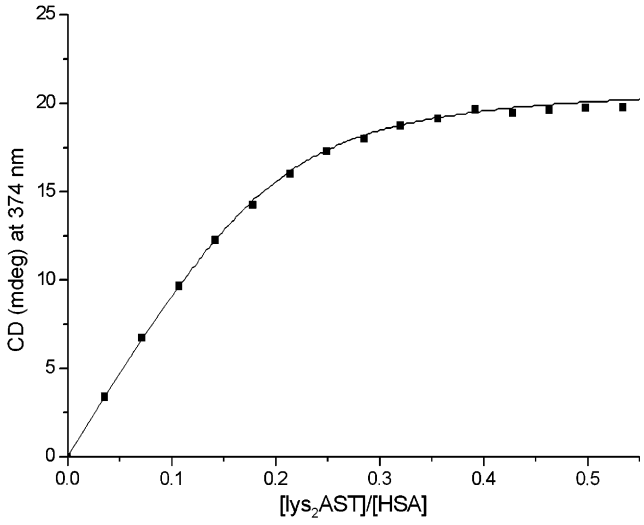

Figure 9. Nonlinear regression analysis (least squares fit) to experimental near-UV CD band intensities (Fig. 6) as a function of *L*/*P* ratios. Values for the binding constant ($K_a = 1.1 \times 10^6\,M^{-1}$) and number of binding sites ($n = 0.20$) are derived.

9.2. Effect of marker ligands on the binding of lys_2AST to HSA evaluated with CD spectroscopy

Several marker ligands were tested as to whether their presence could alter the induced CD signals of monomeric binding of lys_2AST at low *L*/*P* ratios. The binding locations of the ligands utilized were well known, and they do not exhibit induced CD bands in the near UV region. The ligands investigated included *rac*-warfarin (Site I), Na-salicylate (Sites I and II), *rac*-flurbiprofen (Site II), and palmitic acid.

The induced CD of 10 μM lys_2AST binding to 45 μM HSA was recorded in the 280–650 nm range. The biphasic signal belonging to the primary binding of lys_2AST to HSA was unchanged by the addition of *rac*-warfarin and Na-salicylate in the investigated 3:1 and 10:1 *L*/*P* ratios, respectively. However, addition of *rac*-flurbiprofen (up to a 4:1 *L*/*P* ratio) significantly increased both the positive and negative extrinsic CD signals (Fig. 10). Enhancement of the CD amplitudes in the presence of flurbiprofen could not be detected when non-fatty-acid-free HSA was used.

Addition of palmitic acid induced a special effect on the binding of lys_2AST to HSA, as shown in Figure 11. When the ratio of palmitic acid to HSA was 3.85, the induced CD spectra showed only a slight change above 350 nm. Upon further increase of fatty-acid

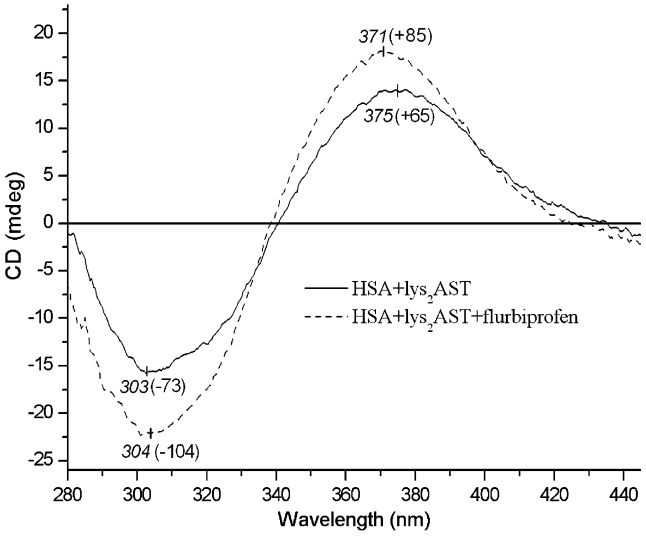

Figure 10. Effect of *rac*-flurbiprofen on the induced CD spectrum of 6.5 μM lys_2AST in 45 μM HSA solution in Ringer buffer, pH 7.4 at 37 °C. Flurbiprofen to HSA molar ratio was 0 (solid line) or 4 (dashed line). Δε values calculated on the basis of total carotenoid concentration are shown in parentheses.

concentration, a substantial change was detected. At palmitic acid to HSA ratios of 4.81 and above, the biphasic Cotton effects at 305 and 374 nm were strongly diminished, with simultaneous development of the familiar positive–negative exciton couplet at 430 and 492 nm suggesting that at higher concentrations of palmitic acid, lys_2AST binding changed from monomeric to aggregated form. This result was supported by a blue shift of the main absorption band. Addition of excess flurbiprofen to the lys_2AST–HSA solution prior to that of palmitic acid resulted in the appearance of the aggregated form at a lower palmitic acid to HSA ratio (3.85) and even more intense excitonic Cotton effects were induced: $\Delta\varepsilon = +86.8$ (495 nm) and -106.1 (430.5 nm).

10. CD and UV–vis spectroscopic investigation of binding of lys_2AST to α_1-acid glycoprotein

UV–vis and CD spectra of 5 and 10 μM lys_2AST obtained in 58 μM AGP solution, together with the spectrum of 15 μM lys_2AST in plain buffer, are shown in Figure 12. The CD and UV–vis curves obtained in AGP solution were similar to those obtained in buffer alone. Therefore, AGP was not effective in prevention of the supramolecular association of lys_2AST, and only weak interaction was suggested.

11. Fluorescence quenching studies

The binding of certain drugs to HSA and AGP can be monitored by following the quenching of the native tryptophan fluorescence of the protein after addition of ligand.[18] We, therefore, studied the effect of lys_2AST on the native fluorescence of HSA and AGP by gradual increase of the ligand concentration in 2 μM protein solutions. Considerable quenching effect was detected in each case (51% with HSA and 44% with AGP at $L/P = 5$), and the profile of the fluorescence quenching curves was quite similar (data not shown). Since the binding of lys_2AST to AGP was postulated to be

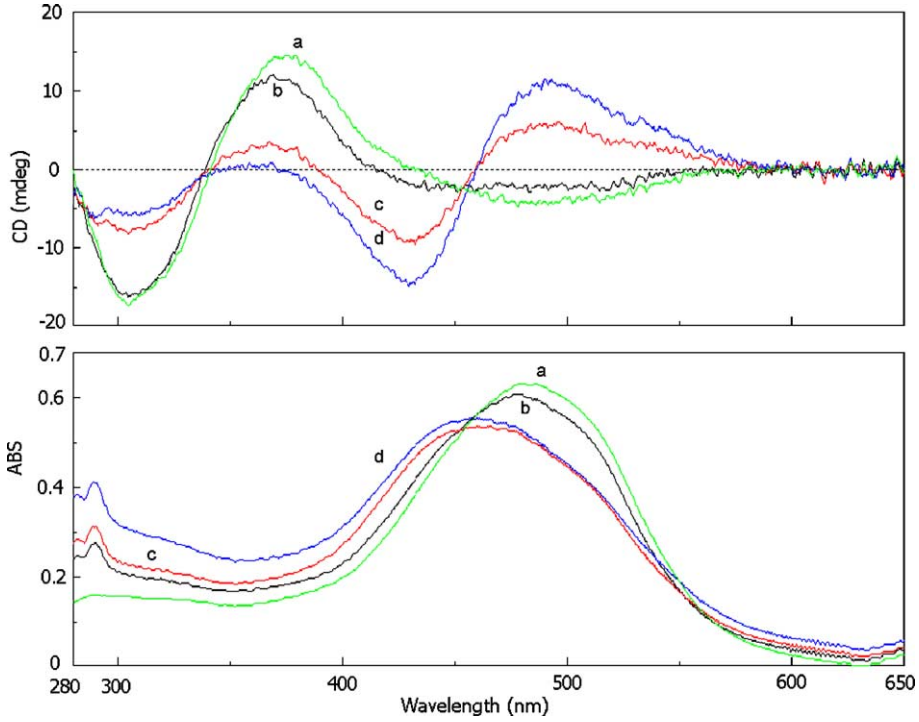

Figure 11. Effect of palmitic acid on the induced CD and UV–vis spectra of 7 μM lys_2AST and 45 μM HSA solution (Ringer buffer, pH 7.4 at 37 °C). Palmitic acid to HSA ratios are 0 (a), 3.85 (b), 4.81 (c), and 5.78 (d). Molar CD intensities of curve (d): at 430 nm $\Delta\varepsilon = -62.2$; at 492 nm $\Delta\varepsilon = +48.7$.

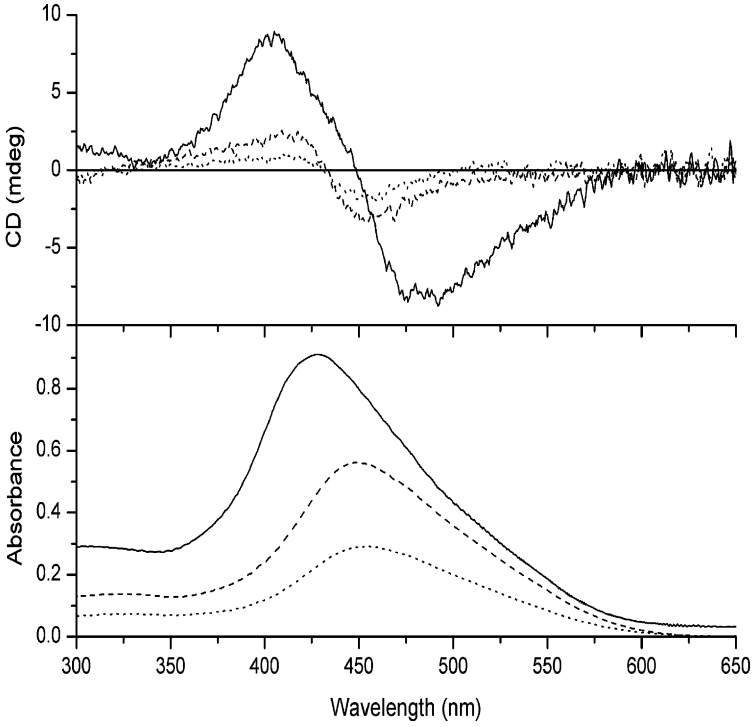

Figure 12. CD and UV–vis spectra of lys_2AST 5 μM (dotted line) and 10 μM (dashed line) in 58 μM α_1-acid glycoprotein solution, and spectra of 15 μM lys_2AST in plain buffer (solid line). (Ringer buffer, pH 7.4 at 37 °C).

significantly weaker than to HSA (see above), the observed fluorescence quenching was attributed to the absorbance of aggregated carotenoid molecules.

12. Discussion

Induced CD spectra obtained at $L/P < 0.4$ demonstrated monomeric binding of lys_2AST to HSA under representative physiologic conditions. The large $\Delta\varepsilon$ values of the positive and negative peaks in the near UV region (Fig. 6) suggested that the binding site strongly preferred a particular chiral conformation of the ligand, in which both terminal ring double bonds are twisted around the C(6)–C(7) and C(6′)–C(7′) bonds in the same direction relative to the planar polyene chain. The optical activity of such a molecule can be interpreted by invoking the so-called 'twisted diene' rule, since there is a relationship between the helicity defined by the end-ring double bonds and the sign of the rotational strengths of the electronic transitions of the polyene chromophore. Accordingly, the negative–positive–negative pattern of the visible and near UV CEs corresponded to the left-handed chiral conformation of the HSA-bound ligand, that is the terminal ring double bonds close a negative torsion angle (the conjugated backbone can formally be treated as a 'single' middle bond as in 1,3-butadiene). The association (binding) constant calculated from the CD titration data suggested high affinity binding, while the stoichiometry of the binding suggested that only a portion of the molecules present in the ligand mixture were subject to Cotton effect-inducing protein binding. While it is likely that only one of the stereoisomers accounted for the observed extrinsic chiral signal, all stereoisomers did in fact bind to HSA—as demonstrated by the lack of any sign of aggregation in the absorption curves.

To obtain more insight into the lys_2AST–HSA interaction, we compared the binding-induced CD spectra of lys_2AST with those previously reported[8] for the disodium disuccinate derivative of *meso*-astaxanthin (dAST):

(a) Monomeric binding of dAST to HSA ($L/P < 0.2$) produced opposite, less intense CEs at considerably longer wavelengths in the near UV region [$\Delta\varepsilon_{max}$ (339 nm) = +23, $\Delta\varepsilon_{min}$ (407 nm) = −25].
(b) Magnitudes of the anisotropy factor ($g = \Delta\varepsilon/\varepsilon$), the concentration-independent measure of molecular chirality, showed notable differences in the two cases: $+3.6 \times 10^{-3}$ (373 nm) and -4.4×10^{-3} (306 nm) for lys_2AST, and -6.0×10^{-4} (402 nm) and $+6.4 \times 10^{-4}$ (341 nm) for dAST, respectively.
(c) While the absorption maximum of dAST showed a bathochromic shift (481 nm ⇒ 496 nm) in the presence of albumin, a similar shift was not observed with the lys_2AST.
(d) $\Delta\varepsilon$ values of the dAST–HSA complex remained constant within the monomeric binding range (no sign of saturation observed), but $\Delta\varepsilon$ values of the lys_2AST steadily decreased with increasing ligand concentration (up to $L/P = 0.6$), indicating saturation of the binding site.
(e) Contrary to the previous observations with dAST, in addition to the chiral aggregation of the carotenoid

molecules on the asymmetric protein host in the range of higher *L*/*P* ratios, monomeric binding-induced Cotton effects of lys_2AST could still be detected at these higher ratios.

These differences emphasized the greater affinity and chiral discriminating power of HSA toward the lysinate derivative. The different wavelength positions of the extrinsic CD and UV–vis peaks of dAST and lys_2AST suggested distinct local microenvironments for the two molecules in the presence of HSA. Since the highly polarizable protein microenvironment is responsible for the bathochromic shift of HSA-bound carotenoid molecules,[8,20] it can be concluded that bound lys_2AST was more accessible to water molecules, while bound dAST was more completely surrounded by the albumin residues. Points (d) and (e) above suggested that while dAST interacted with the same region of HSA both as a monomer and in aggregated form, different locations existed for lys_2AST monomer binding and HSA-induced chiral aggregation.

These results are most likely related to the different physicochemical properties of the two ligands:

- lys_2AST and dAST are oppositely charged (cationic and anionic, respectively) at physiologic pH;
- the L-lysine moiety has an asymmetric center that may contribute to the molecular recognition process at the protein binding site;
- lys_2AST may establish stronger noncovalent interactions with the binding environment due to simultaneous hydrogen donor and acceptor abilities of the lysine moieties.

The displacement experiments performed with site marker ligands of HSA demonstrated that lys_2AST bound to neither of the main albumin drug binding sites. Moreover, the monomeric binding site of lys_2AST was allosterically influenced by flurbiprofen and palmitic acid in different directions. Flurbiprofen increased the monomeric binding of the ligand, while an excess of fatty acid diminished monomeric binding with a simultaneous increase of aggregate binding. The positive cooperative interaction was presumably caused by the secondary binding of flurbiprofen to HSA, the high-affinity primary binding of which occurs at drug-binding Site II on HSA.[21] The flurbiprofen-mediated binding enhancement of lys_2AST was not observed with non-fatty-acid-free albumin, suggesting that the secondary binding location of flurbiprofen was identical to a palmitic acid binding site. The complex effect of palmitic acid may be explained by the dramatic conformational change of HSA upon fatty acid binding, as demonstrated in X-ray studies;[22] widening of the central crevice (interdomain cleft) of HSA was favorable for accommodating the chiral lys_2AST aggregate. The exact location of the monomeric binding site for lys_2AST, indeterminate from the current set of experiments, might be amenable to X-ray crystallographic experiments.

The cationic carotenoid derivative astaxanthin dilysinate tetrahydrochloride formed H-type (card-pack) aggregates in aqueous solution, and bound to HSA with high affinity. It did not form precipitates in the presence of albumin in vitro. At low ligand per protein ratios, monomeric binding occurred, which did not interfere with established main drug binding sites (Sites I and II) on HSA. At higher *L*/*P* ratios, the carotenoid molecules formed aggregates on the asymmetric protein host, most likely in the large central crevice of HSA.

The presence of an excess of fatty acids allosterically favored aggregate binding. The chiral binding stoichiometry, as determined by CD spectroscopy, was approximately 0.20–0.24 per HSA molecule suggesting that only one of the stereoisomers of the lys_2AST was subject to protein-induced chiral signals. Only weak binding of the test ligand to AGP was observed in the current study.

Acknowledgements

The authors wish to thank members of Albany Molecular Research, Inc. (AMRI) for support on chemical synthesis, analytical separation, and characterization of the test ligand (Dean A. Frey Ph.D., Mark McClaws Ph.D., Qiang Yang Ph.D., and Juris L. Ekmanis Ph.D.). A. J. Cardounel and Jay L. Zweier (Davis Heart & Lung Institute, Columbus, Ohio) participated in early scavenging experiments with the test ligand, providing preliminary evidence of the H-type ('card-pack') aggregation of the compound. Hans-Richard Sliwka, Vassilia Partali, Bente Foss, Thor-Bernt Melø, and Razi Naqvi (NTNU-Trondheim, Norway) provided ongoing insight into water-dispersible carotenoids. We thank Júlia Visy for chiral HPLC measurements (Chemical Research Center, Hungary). David M. Watumull assisted with manuscript and figure preparation and submission of the final manuscript.

References and notes

1. *Carotenoids: Isolation and Analysis*; Britton, G., Liaaen-Jensen, S., Pfander, H., Eds.; Birkhäuser: Basel, 1995; Vol. Ia, pp 81–108.
2. *Carotenoid Handbook*; Britton, G., Liaaen-Jensen, S., Pfander, H., Mercadante, A. Z., Egeland, E. S., Eds.; Birkhäuser: Basel, 2004.
3. Bertram, J. S. *Nutr. Rev.* **1999**, *57*, 182–191.
4. Lockwood, S. F.; O'Malley, S.; Mosher, G. L. *J. Pharm. Sci.* **2003**, *92*, 922–926.
5. Williams, A. W.; Boileau, T. W.; Clinton, S. K.; Erdman, J. W., Jr. *Nutr. Cancer* **2000**, *36*, 185–190.
6. Foss, B. J.; Naess, S. N.; Sliwka, H. R.; Partali, V. *Angew. Chem., Int. Ed.* **2003**, *42*, 5237–5240.
7. Cardounel, A. J.; Dumitrescu, C.; Zweier, J. L.; Lockwood, S. F. *Biochem. Biophys. Res. Commun.* **2003**, *307*, 704–712.
8. Zsila, F.; Simonyi, M.; Lockwood, S. F. *Bioorg. Med. Chem. Lett.* **2003**, *13*, 4093–4100.
9. Gross, G. J.; Lockwood, S. F. *Life Sci.* **2004**, *75*, 215–224.
10. Showalter, L. A.; Weinman, S. A.; Østerlie, M.; Lockwood, S. F. *Comp. Biochem. Physiol. C: Pharmacol. Toxicol.* **2004**, *137*, 227–236.
11. Hix, L. M.; Lockwood, S. F.; Bertram, J. S. *Cancer Lett.* **2004**, *211*, 25–37.

12. Foss, B. J.; Sliwka, H. R.; Partali, V.; Cardounel, A. J.; Zweier, J. L.; Lockwood, S. F. *Bioorg. Med. Chem. Lett.* **2004**, *14*, 2807–2812.
13. Jackson, H. L.; Cardounel, A. J.; Zweier, J. L.; Lockwood, S. F. *Bioorg. Med. Chem. Lett.* **2004**, *14*, 3985–3991.
14. Bikádi, Z.; Zsila, F.; Deli, J.; Mady, G.; Simonyi, M. *Enantiomer* **2002**, *7*, 67–76.
15. Simonyi, M.; Bikadi, Z.; Zsila, F.; Deli, J. *Chirality* **2003**, *15*, 680–698.
16. He, X. M.; Carter, D. C. *Nature* **1992**, *358*, 209–215.
17. Fitos, I.; Visy, J.; Simonyi, M.; Hermansson, J. *Chirality* **1999**, *11*, 115–120.
18. Parikh, H. H.; McElwain, K.; Balasubramanian, V.; Leung, W.; Wong, D.; Morris, M. E.; Ramanathan, M. *Pharm. Res.* **2000**, *17*, 632–637.
19. Petitpas, I.; Bhattacharya, A. A.; Twine, S.; East, M.; Curry, S. *J. Biol. Chem.* **2001**, *276*, 22804–22809.
20. Zsila, F.; Bikádi, Z.; Simonyi, M. *Tetrahedron: Asymmetry* **2001**, *12*, 3125–3137.
21. Honore, B.; Brodersen, R. *Mol. Pharmacol.* **1984**, *25*, 137–150.
22. Curry, S.; Brick, P.; Franks, N. P. *Biochim. Biophys. Acta* **1999**, *1441*, 131–140.